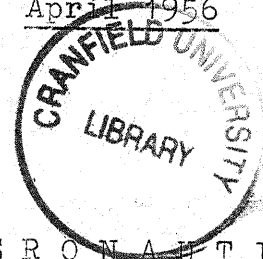




ST. NO. 2R 788  
U.D.C.  
AUTH.

Note No. 44  
April 1956

CONFIDENTIAL



THE COLLEGE OF AERONAUTICS  
CRANFIELD

Aerodynamic Characteristics of two low  
aspect ratio rectangular wings at Mach number 2.

---

Preliminary report and summary of results.

by

G. B. Marson.

(Issued under Ministry of Supply Contract M.o.S. 7/Exptl/571/R3)

PDF

This note summarises the more important results of a detailed experimental investigation into the flow and pressure distribution over two rectangular single wedge wings. The experiments were carried out in the 9" x 9" supersonic tunnel at the College of Aeronautics, at a Mach number of 2.0 and a Reynolds number of  $2.5 \times 10^6$  per foot. Both wings had a chord of 3 inches and a total wedge angle of  $6^\circ$ . They had no real trailing edge, but were faired into a cylindrical support which could be rolled and pitched in the tunnel. Wing A was of 2 inch span, giving an aspect ratio of 0.67. Wing B was of  $1\frac{1}{4}$  inch span, 0.42 aspect ratio. 132 pressure tappings were spaced regularly over half of one surface of each wing, and up to 19 pressure readings could be taken simultaneously on vertical mercury manometers. The models were pressure plotted at pitch angles of  $0^\circ$ ,  $2\frac{1}{2}^\circ$ ,  $5^\circ$ ,  $7\frac{1}{2}^\circ$ ,  $10^\circ$ ,  $15^\circ$ ,  $20^\circ$ ,  $25^\circ$ , and  $30^\circ$ , and at all roll angles at intervals of  $30^\circ$ . Since each wing was symmetrical about the centreline, the complete pressure distribution over all surfaces at any roll angle  $\phi$  could be obtained from the readings taken on the one surface at  $\phi$ ,  $180^\circ - \phi$ ,  $180^\circ + \phi$ , and  $360^\circ - \phi$ . The pressure readings were then integrated to give the forces and moments on the complete wing.

A large number of Schlieren and surface flow photographs were also taken, to give detailed information on the flow patterns and vortex formations involved. A full report of the results of the visualisation tests and pressure plotting is in course of preparation. This note presents only the integrated force and moment results.

The attitude of the model was determined by a pitch  $\theta$ , about the horizontal wind axis, and a roll  $\phi$  about its own centreline, but the force results are presented in terms of the angles of incidence  $\alpha$ , and sideslip  $\beta$ , where

$$\tan \alpha = \tan \theta \cos \phi \text{ (tangent definition)}$$

$$\sin \beta = \sin \theta \sin \phi \text{ (sine definition)}$$

## Results and Conclusions

### 1. Pressure distributions at $0^\circ$ roll.

The pressure coefficients generally were not linear with incidence and the low incidence results gave only fair agreement with linearised theory (Gunn). Pressures

on the lower (pressure) surface were considerably higher than those predicted by linearised theory, but near the leading edge all the pressure coefficients agreed reasonably well with shock-expansion values. The region of negative lift expected behind the first Mach wave reflection on Wing B was not found, although the upper surface suction did become very small or negative towards the trailing edge. When the incidence was increased above  $20^\circ$ , the suction values tended to remain constant as the value corresponding to absolute vacuum ( $C_p = -0.36$ ) was approached. The combination of this effect and the 'positive' non-linearity on the lower surface pressures, resulted in a normal force curve which was practically linear at high incidences (Figure 1).

The spanwise pressure distributions are shown as integrated values for each chordwise column of pressure tappings, in figures 2, 3 and 4. The lower surface pressures give an almost elliptical distribution, as expected, and the upper surface suction shows clearly the effect of the tip vortex at incidences above  $7\frac{1}{2}^\circ$ , by an increase of suction towards the tip. (Apart from this effect, the upper surface pressure coefficients are, surprisingly, more linear than those on the lower surface.) The resulting lift distribution is practically constant in the spanwise direction up to high angles of incidence.

## 2. Normal Force, lift and drag at $0^\circ$ roll.

The normal force curve slope at zero incidence for wing A agrees well with linearised theory, and remains reasonably linear between  $10^\circ$  and  $25^\circ$  incidence (figure 1). Linearised theory for Wing B predicts a much reduced normal force (due to the theoretical negative lift region), but this is not borne out by experiment. The discrepancies are not, as might be expected, due directly to tip vortex effects, but originate in the large lower surface pressures. However, the non-linear lift on Wing A agrees well with Flax and Lawrence's empirical result

$$C_N = \left( \frac{\partial C_N}{\partial \alpha} \right)_{\alpha=0} \alpha + 2\alpha^2.$$

The lift and drag curves (figures 5 to 8) are derived from the normal force results

$$\begin{aligned} \text{viz. } C_L &= C_N \cos \alpha \\ C_D &= C_N \sin \alpha \cos \beta. \end{aligned}$$

The deviations from linearised theory reflect those found in the normal force.

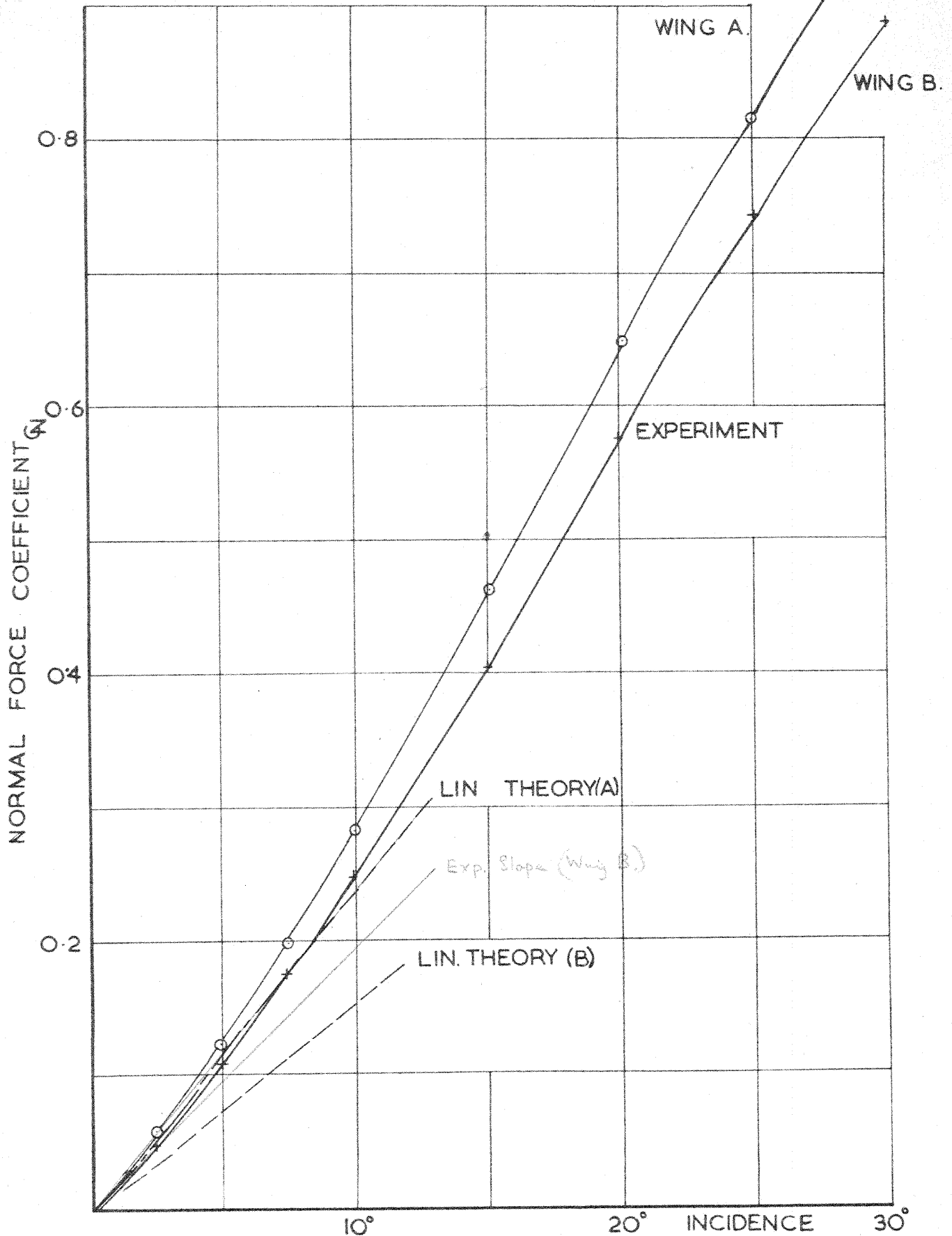
3. Effect of roll or sideslip.

Figure 4 shows the effect of sideslip on the spanwise pressure distribution at  $10^\circ$  pitch. The lower (windward) tip vortex is swept inboard, on to the wing, causing an increase of suction near the lower tip. Similarly there is a decrease of suction near the upper tip, resulting in a restoring rolling moment in all cases (figure 12). However, the lower surface pressures also increase appreciably over the whole of the lower half-wing and it is found that the total normal force and lift on both wings increase slightly as the angle of sideslip increases (figures 5 and 6).

4. Centre of Pressure position and Rolling Moment.

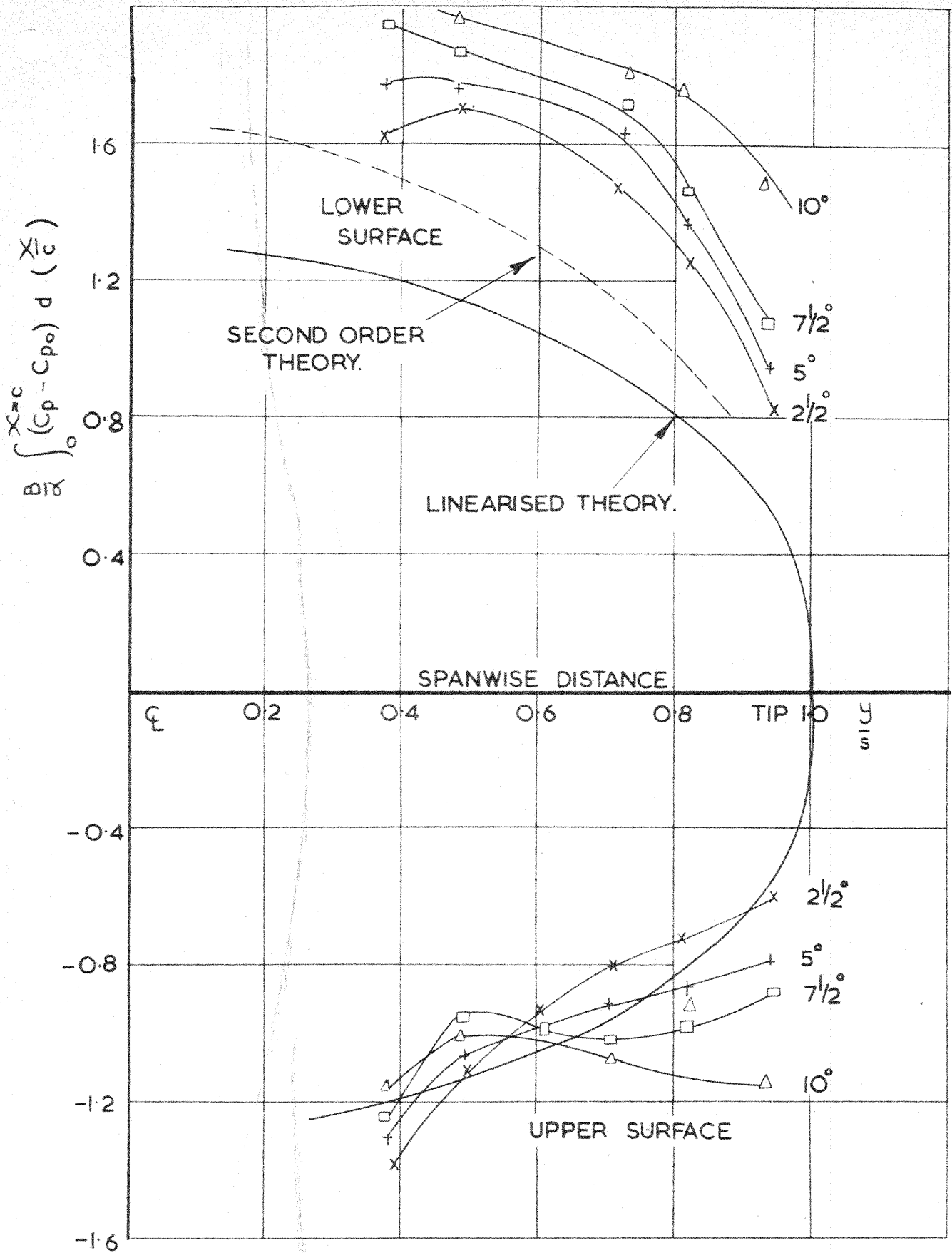
The movement of the centre of pressure with incidence at zero roll is shown in figure 9. Below  $5^\circ$  the accuracy of the results is no better than  $\pm 0.02$ , owing to the small forces and moments involved.

As can be seen, the chordwise centre of pressure position moves aft rapidly as the incidence is raised to  $10^\circ$ , but thereafter the effect is much reduced. At roll, the change in pressure distribution already discussed causes the spanwise centre of pressure position on each half-wing to move to windward. The effect is greater on wing B, and the resulting rolling moment on this wing is about twice that on wing A. The effect of roll on the chordwise co-ordinate is to shift the centre of pressure aft on the lower (windward) half-wing and forward on the upper half-wing. This is explained by the increased effect at roll of the lower tip vortex, which is predominant on the rear half of the wing.

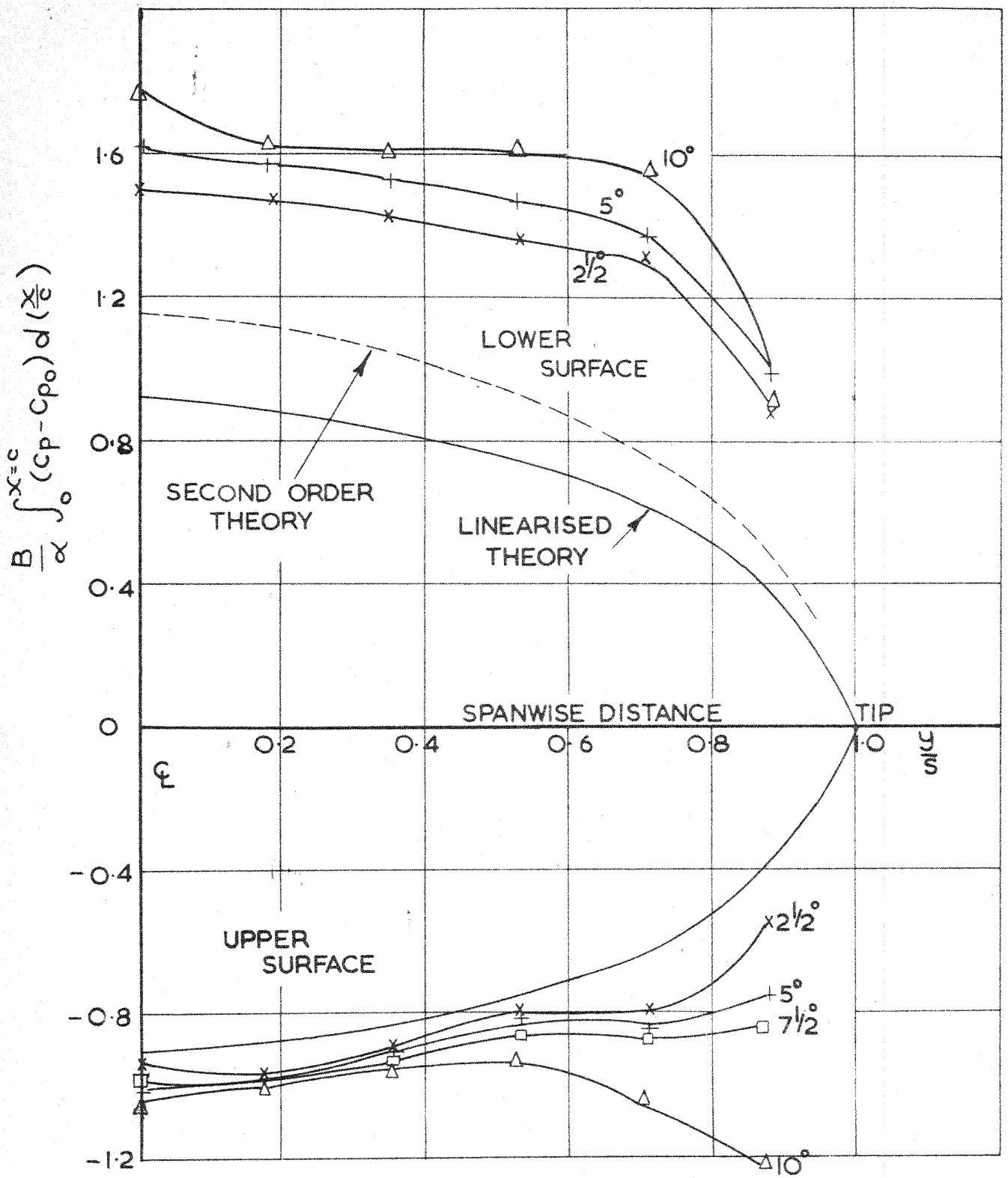


VARIATION OF NORMAL FORCE WITH  
INCIDENCE AT ZERO ROLL ANGLE

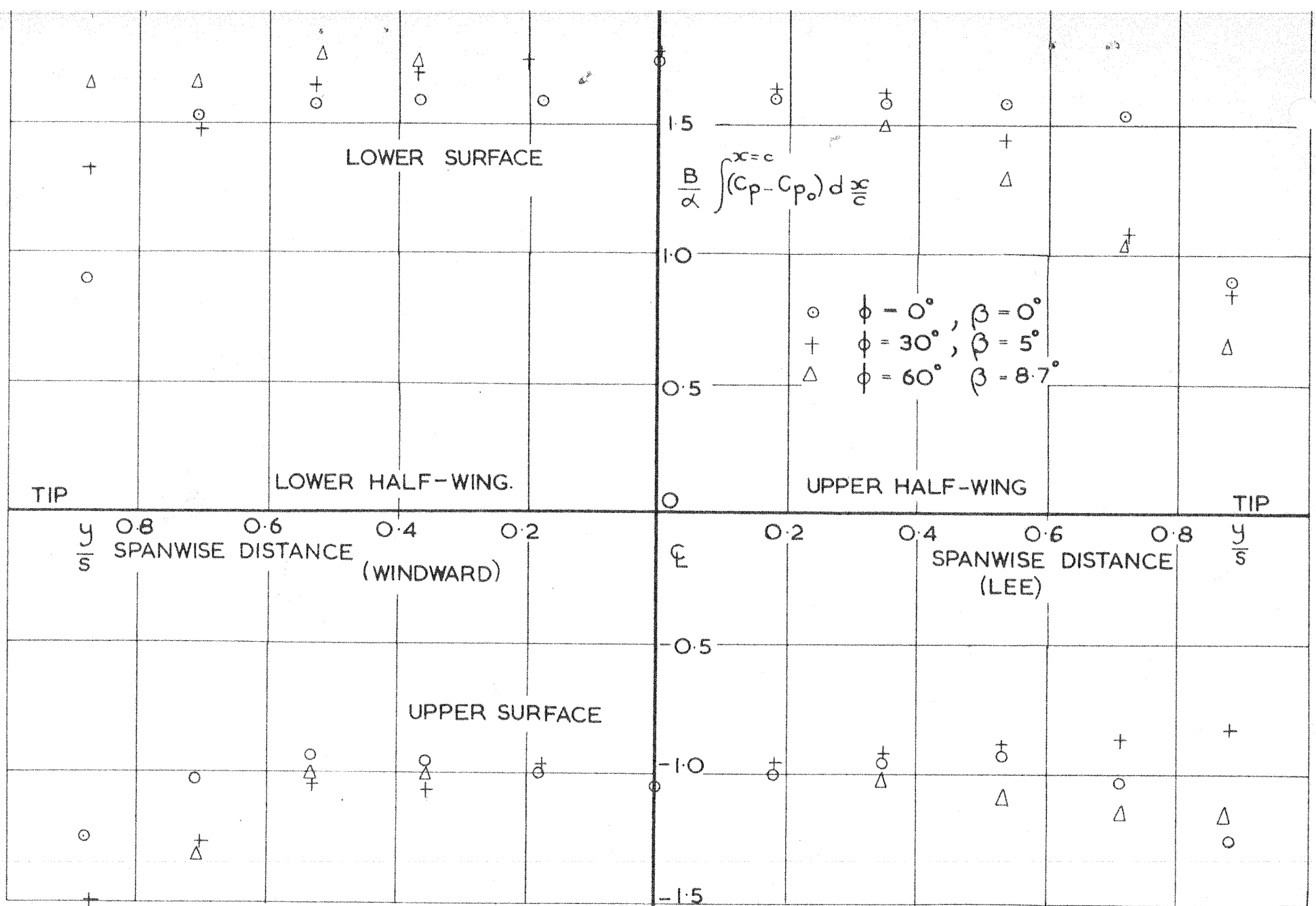
FIG1



SPANWISE DISTRIBUTION OF PRESSURE ON EACH SURFACE WING A. FIG.2

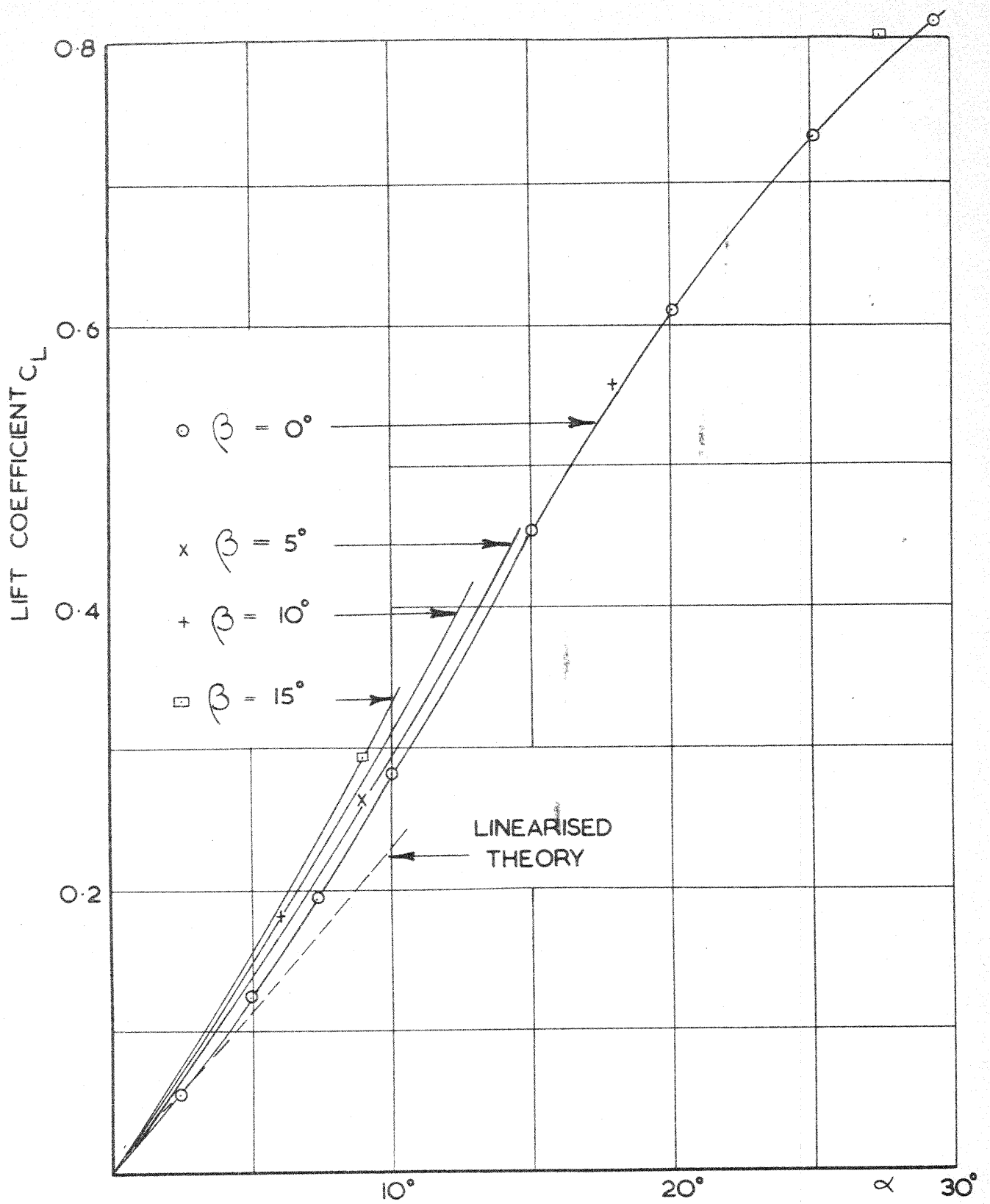


SPANWISE DISTRIBUTION OF PRESSURE ON EACH SURFACE WING B. FIG.3



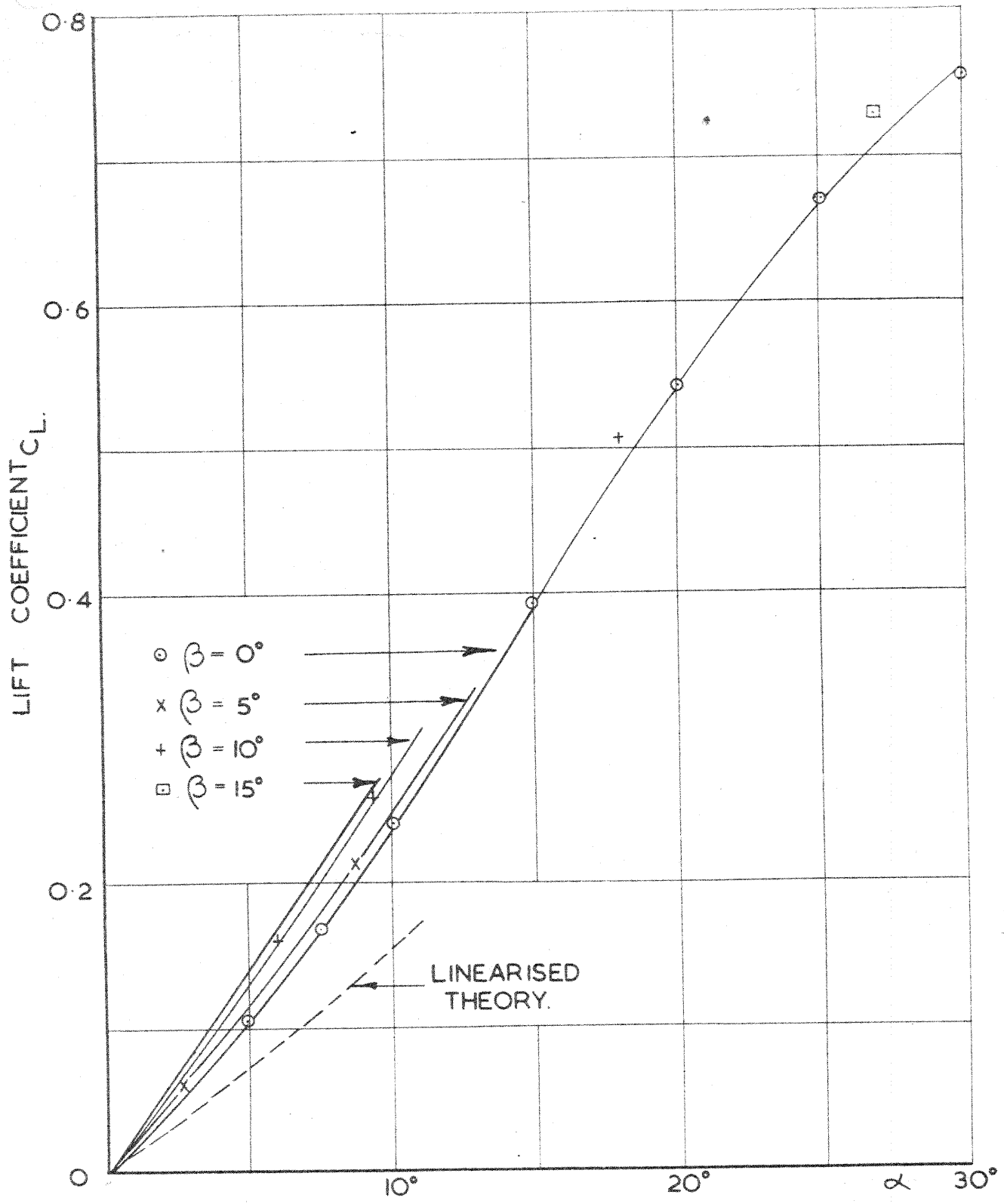
SPANWISE DISTRIBUTION OF PRESSURE ON EACH SURFACE  
AT VARIOUS ROLL ANGLES. WING B.(10° PITCH).





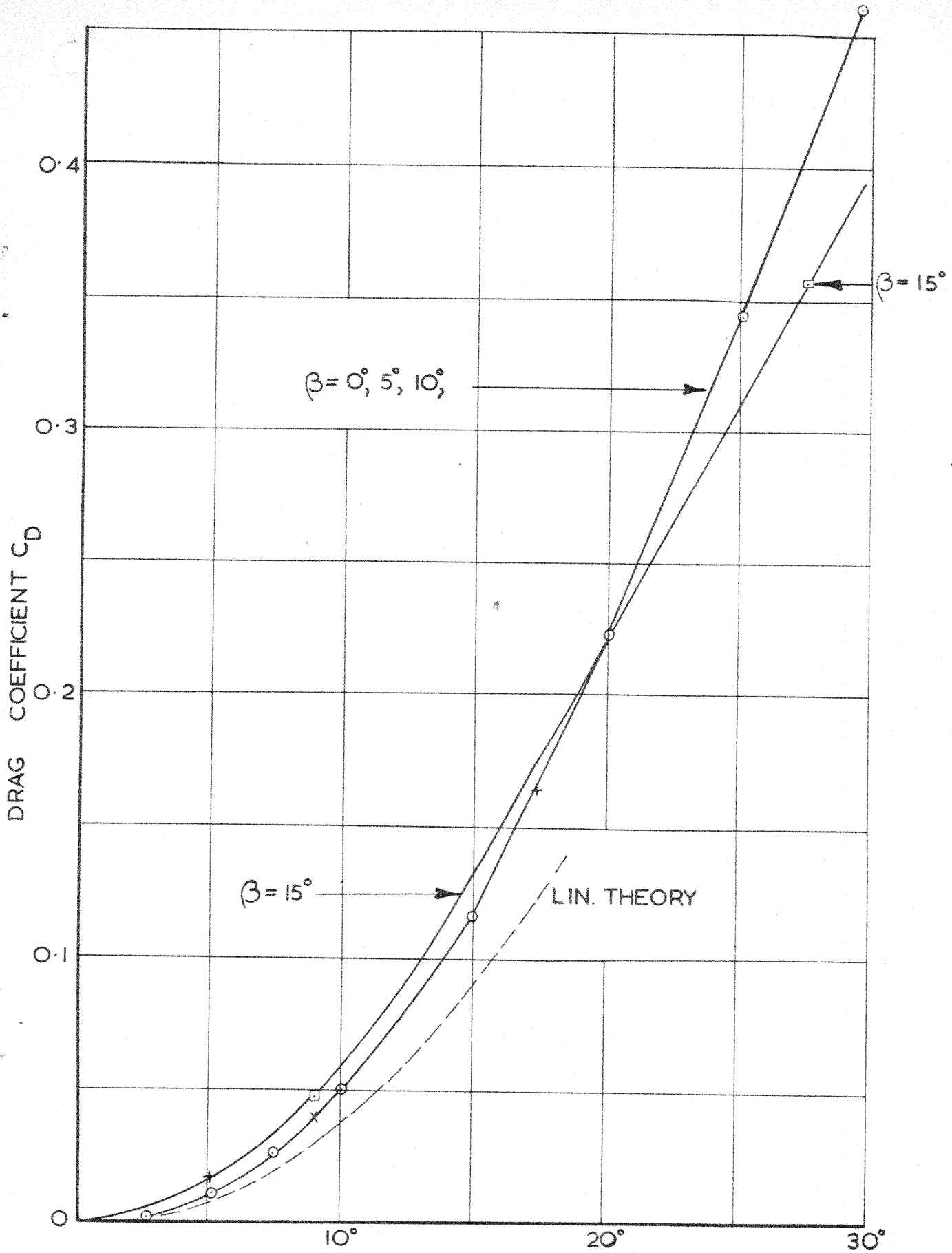
VARIATION OF LIFT COEFFICIENT WITH INCIDENCE & SIDESLIP. WING A.

FIG. 5



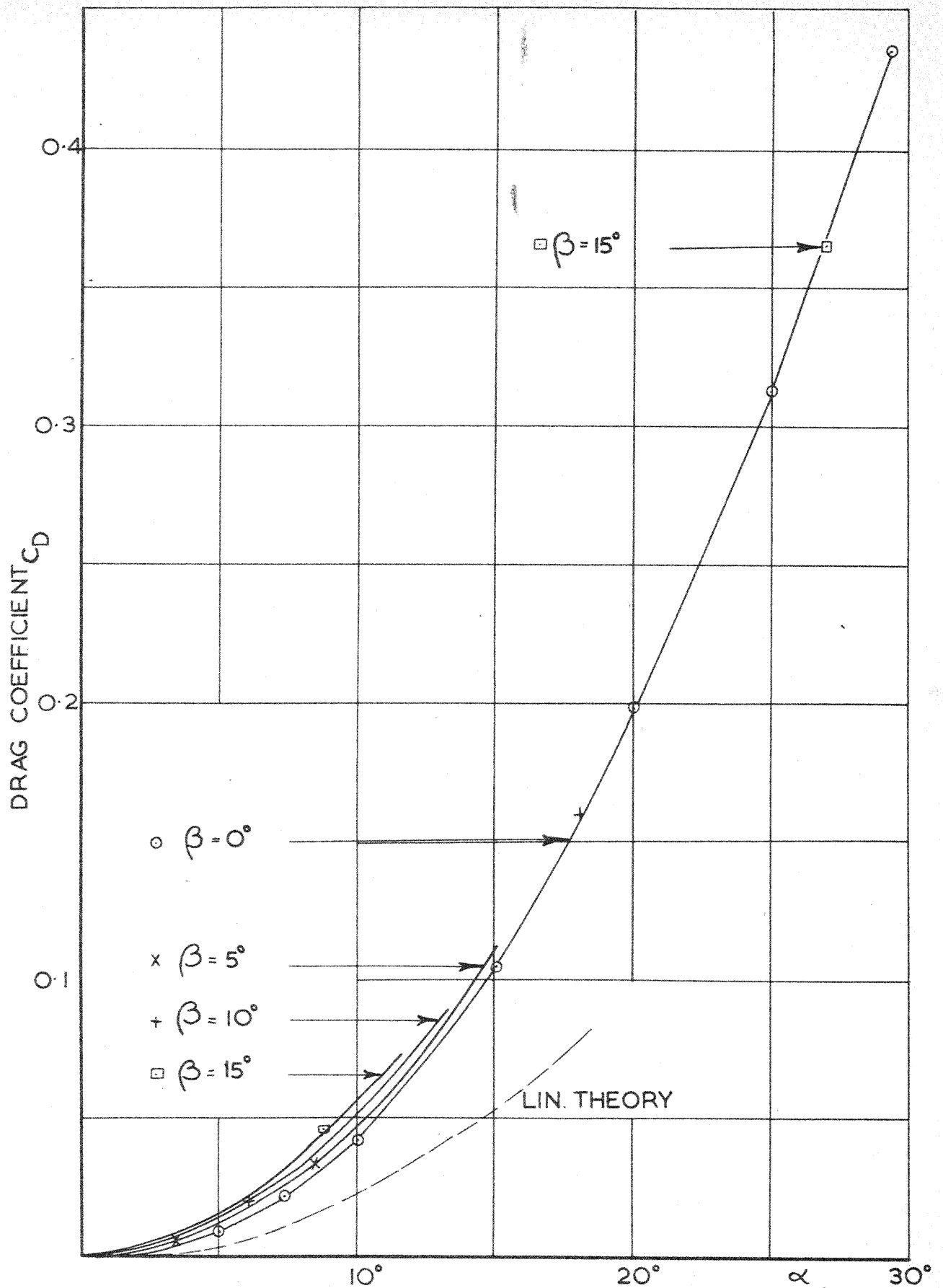
VARIATION OF LIFT COEFFICIENT WITH INCIDENCE & SIDESLIP. WING B.

FIG.6



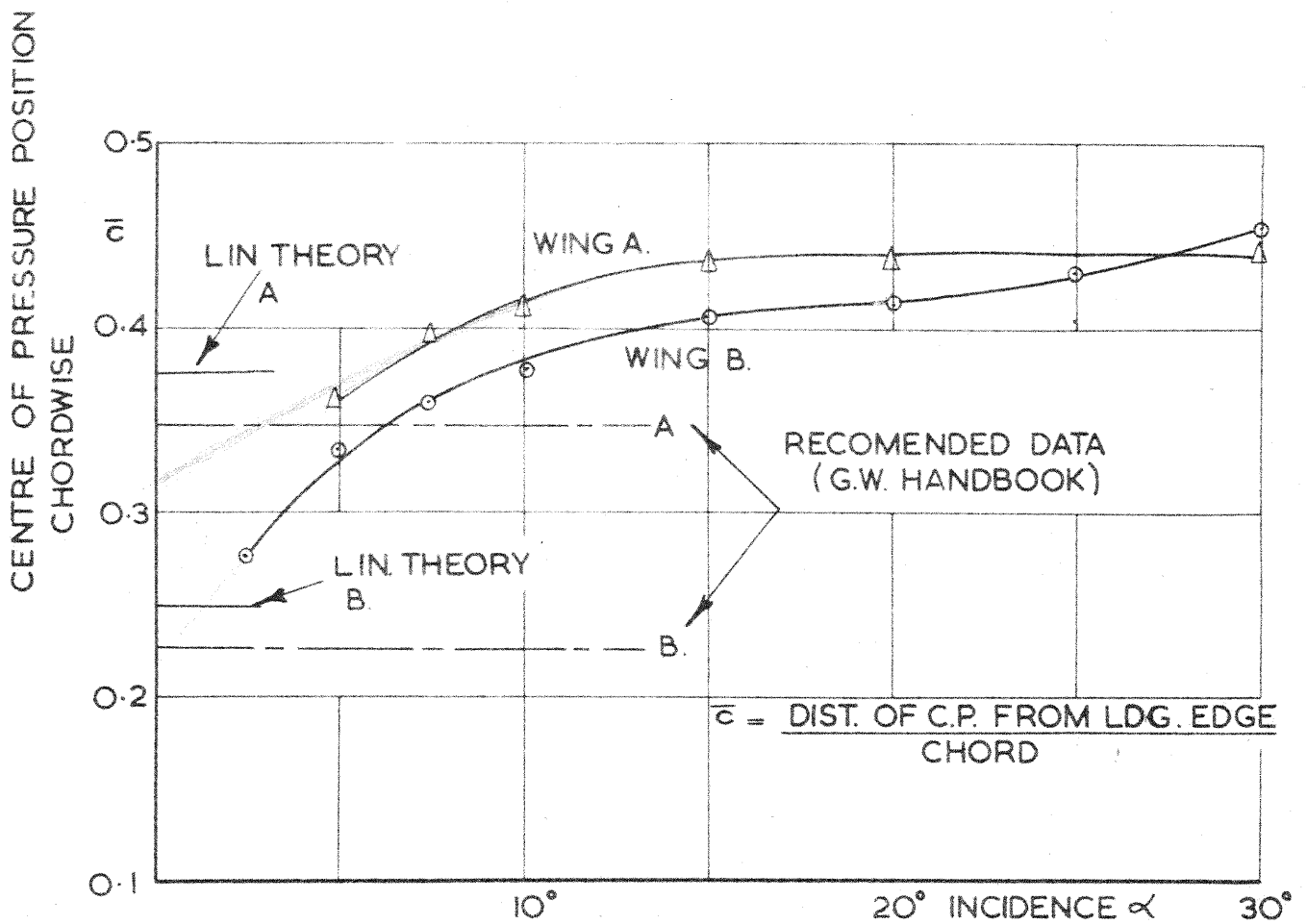
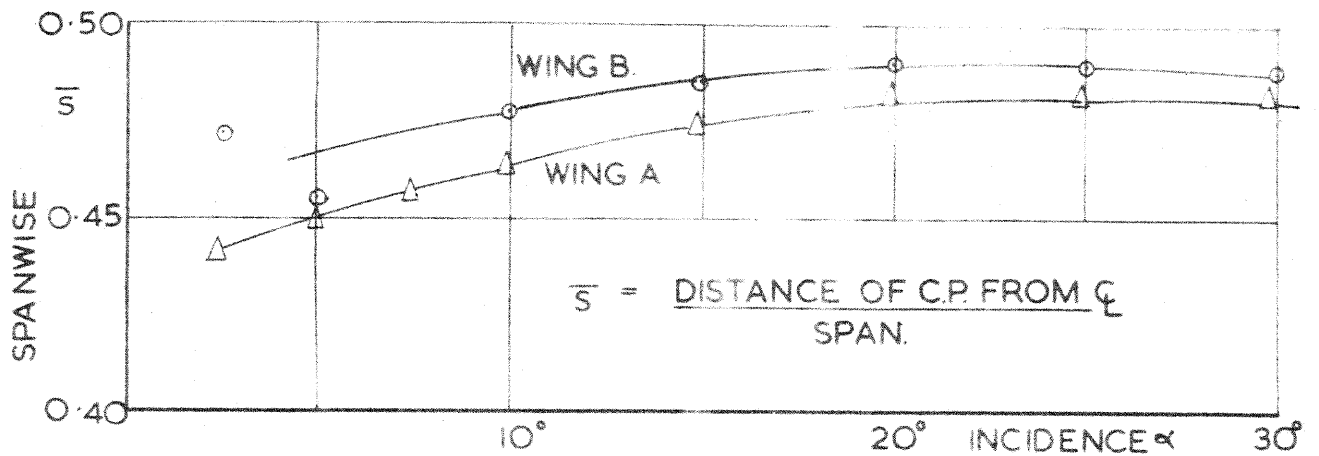
VARIATION OF DRAG COEFFICIENT WITH INCIDENCE & SIDESLIP WING.A.

FIG.7



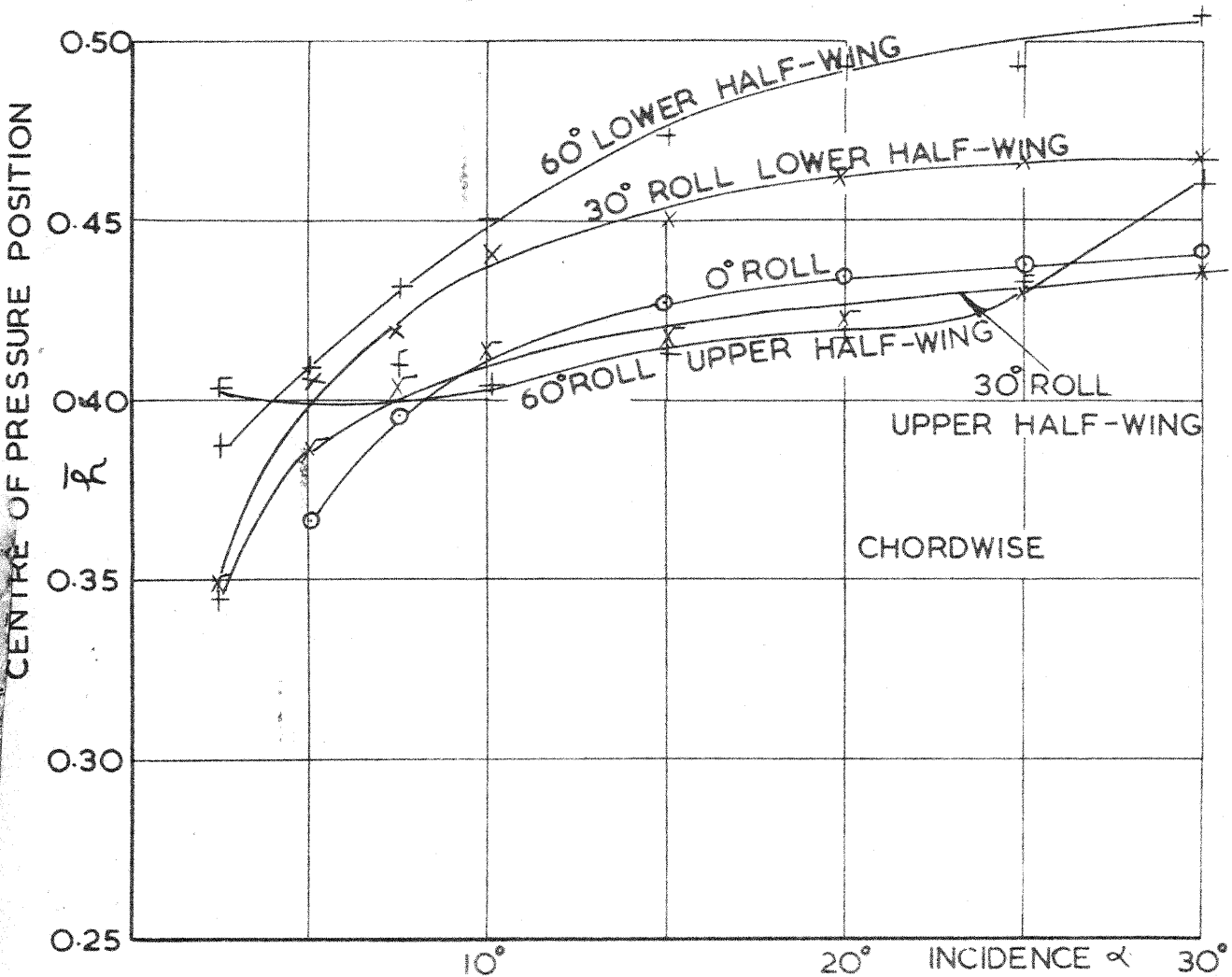
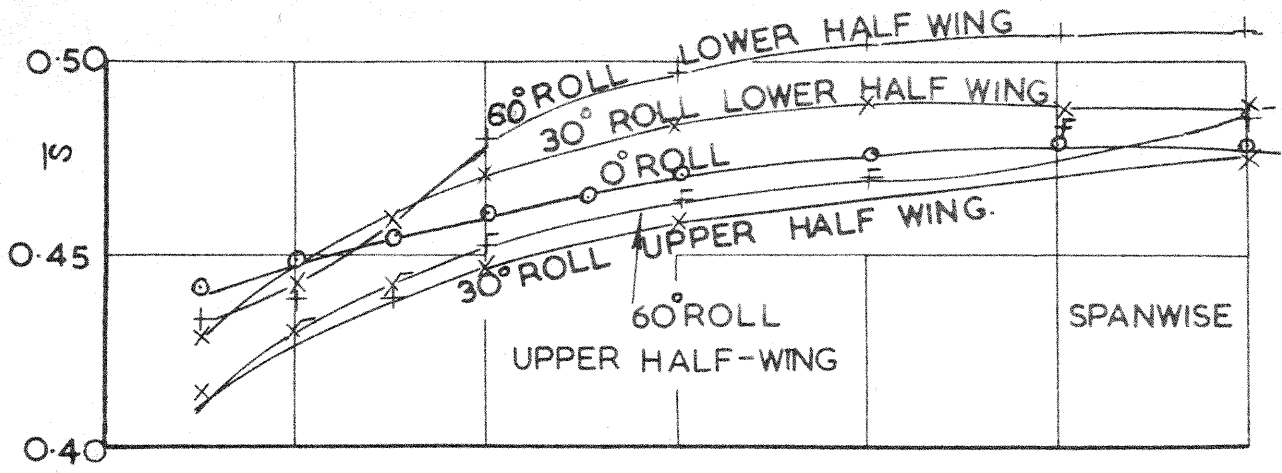
VARIATION OF DRAG COEFFICIENT WITH INCIDENCE & SIDESLIP. WING B.

FIG.8



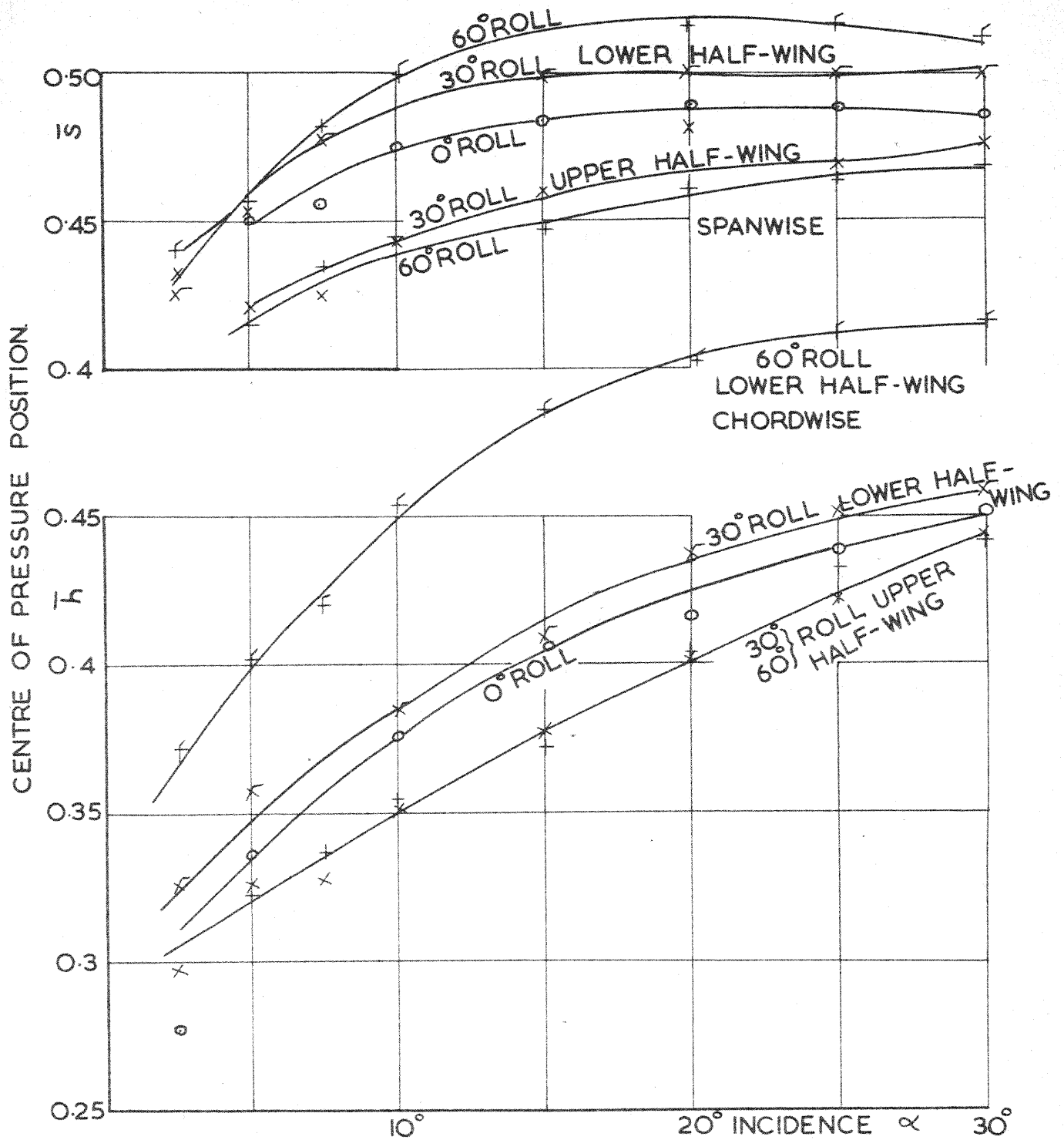
SPANWISE & CHORDWISE CO-ORDINATES OF CENTRE OF PRESSURE AT ZERO ROLL.

FIG.9



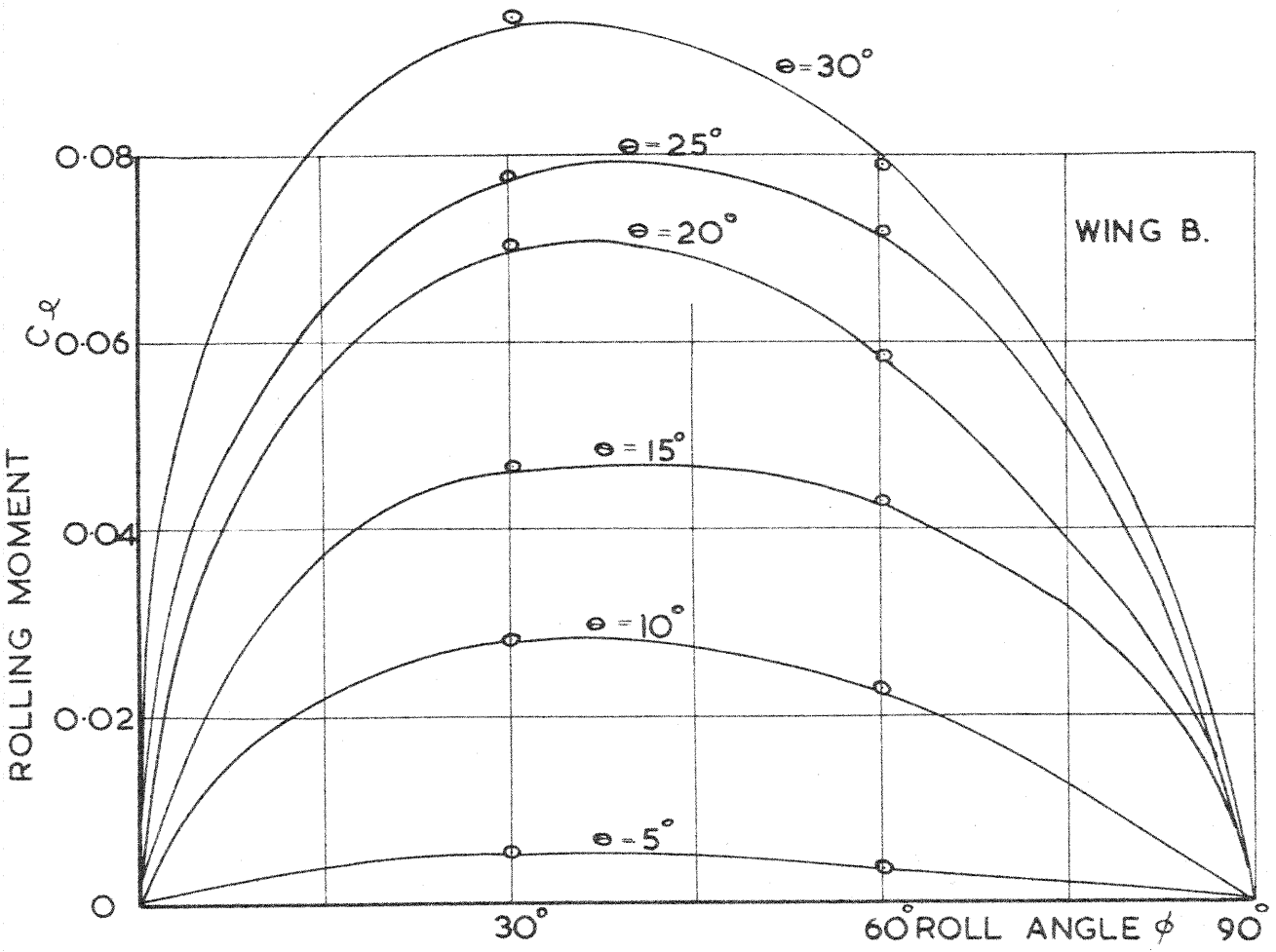
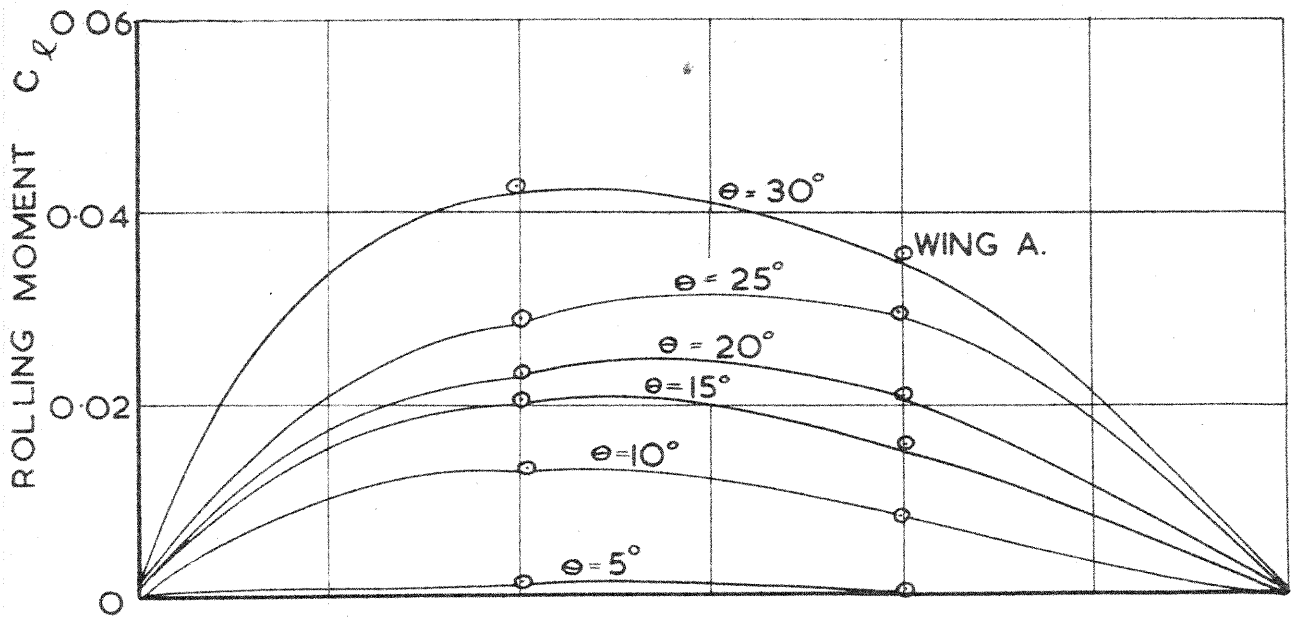
SPANWISE & CHORDWISE CO-ORDINATES OF CENTRE OF PRESSURE AT VARIOUS ROLL ANGLES. WING A.

FIG.10



SPANWISE & CHORDWISE CO-ORDINATES OF CENTRE OF PRESSURE AT VARIOUS ROLL ANGLES.

FIG.II



VARIATION OF ROLLING MOMENT WITH ANGLES OF ROLL & PITCH.

FIG.12